First-order unbinding transition of an interface in two dimensions

G. Forgacs, N. M. Švrakić, and V. Privman
Department of Physics, Clarkson University, Potsdam, New York 13676
(Received 25 February 1988)

A two-dimensional model describing the unbinding of an interface from an attracting substrate, induced by a defect line in the bulk, is proposed. It contains Abraham's model as a special case. Although only short-range interactions are present, a sharp first-order unbinding transition is shown to take place. The model is formulated in terms of both the solid-on-solid model and Ising spins. Thermodynamic properties are evaluated exactly in both cases. The average interface distance from the substrate and the full magnetization profile are calculated in the solid-on-solid version. The first-order transition is discussed in light of Cahn's wetting criterion.

I. INTRODUCTION

The behavior of an interface in the presence of an attracting substrate is a subject of considerable interest.[1] One of the most extensively studied phenomena in this field is wetting.[2] Most of the analytic studies of wetting transitions (interface unbinding) are based on models with power-law long-range forces. This is motivated by the fact that systems with experimentally observed first-order wetting transition involve some kind of long-range forces. The exactly solvable two-dimensional (2D) model of Abraham[3] (model A), which contains only short-range forces, leads to a continuous wetting transition.

In the present work we introduce and solve exactly a 2D model (model AB), with short-range forces, which exhibits a sharp first-order unbinding transition. Exact solutions for first-order transitions, as opposed to second-order transitions[4] are scarce. Furthermore, finite-size scaling theory for first-order phase transitions[5] has not been tested in exactly solvable models, except for the mean-field theory. Our new model AB will be solved analytically for finite-size effects.

We will formulate the new model both in terms of Ising spins and the restricted solid-on-solid (RSOS) model. The 2D Ising version of the model is depicted in Fig. 1. The substrate is represented by the boundary with negative spins. The contact interaction attracting the interface to the substrate is modeled by a line of weak bonds $J_1=a_1J$ $(0\le a_1\le 1)$, where J denotes the bulk ferromagnetic interaction. The boundary conditions far from the substrate, in the Nth layer select positive spins. At a distance L from the substrate a second line of attracting bonds $J_2=a_2J$ $(0\le a_2\le 1)$ is introduced. With $a_2=1$, i.e., in the absence of the second defect line, the system is known as the Abraham's model (model A). It undergoes a continuous wetting transition at a temperature T_w below the critical temperature (T_c) of the 2D Ising model. At the wetting transition the average distance of the interface (separating the predominantly + and − phases) from the substrate diverges smoothly to infinity. The profile of the magnetization, $m(z)$, measured from the substrate at $z=0$, changes sign at $z_0(T)$. As the transition temperature is approached from below, z_0 diverges continuously.

The introduction of the second line of weak (defect) bonds, J_2, at a distance L from the substrate changes drastically the above picture. In the limit $L\to\infty$ $(L\ll N)$, and provided $a_2>a_1$, the interface unbinds discontinuously from the substrate and becomes localized at the second defect line. This first-order transition takes place at $T_1\le T_w$. At T_1 the distance of the interface from the substrate, represented by z_0, jumps from a finite value to infinity. For finite but large L the transition is rounded. Since we are able to perform an explicit calculation for finite L, we can verify the predictions of the finite-size scaling theory.

Finally, in our terminology the case with $a_1=1$ and with a defect line in the bulk corresponds to model B, discussed in Refs. 3 and 6. Since this model does not exhibit

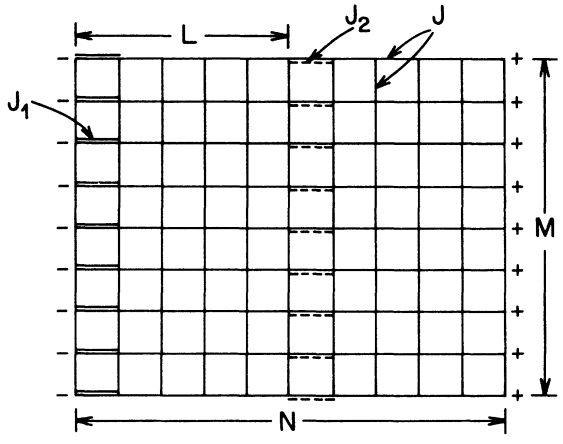

FIG. 1. 2D Ising model with nearest-neighbor ferromagnetic couplings J (solid lines) and two seams of defects: one with couplings $J_1=a_1J$ (double-solid lines) positioned next to the substrate (− edge) and the other with couplings $J_2=a_2J$ (solid-dashed lines) at a distance L from the substrate. Both $a_1,a_2\le 1$. Case $a_1<a_2<1$ corresponds to model AB; $a_1<1$, $a_2=1$ to model A; and $a_1=1$, $a_2<1$ to model B.

a wetting transition, it is of no immediate interest to us.

This paper is organized as follows. In Sec. II, we present the formalism[6] for calculating the free energy of model AB in the Ising language. In Sec. III we consider the particular case of $a_2=1$, model A.[3] Section IV describes the results for $a_1<a_2<1$ in the limit $L\to\infty$, while in Sec. V we study the effects of finite L. In Sec. VI, the RSOS version of model AB is described and its free energy is calculated. In Secs. VII and VIII, respectively, we obtain analytic results for the average interface displacement and magnetization profile of the RSOS model. We conclude (Sec. IX) with a summary and a discussion of the results, including the connection of our first-order unbinding transition with Cahn's wetting criterion.[7]

II. EXACT RESULTS FOR THE 2D ISING MODEL WITH BULK AND SURFACE DEFECT LINES

To calculate the interfacial properties of the Ising model depicted in Fig. 1 we use the transfer matrix method. Denote, by $|+\rangle$ and $|-\rangle$, the column states with all spins up or down, respectively. Then the partition function of model AB can be expressed as

$$Z_{+-}=\langle +|V^{N-L}W_2V^{L-1}W_1|-\rangle\ . \tag{2.1}$$

Here V, W_1, and W_2 are the transfer matrices of the 2D Ising model with interactions J, J_1, and J_2, respectively. [We take the horizontal size of the system to be $N+2$, which explains the exponents in (2.1). This will not matter in the $N\to\infty$ limit.] In order to cast (2.1) in form of a trace, customary in transfer matrix calculations, we introduce a complete set of column states $|\nu\rangle$ and write

$$Z_{+-}=\sum_{\nu}\langle\nu|V^{L-1}W_1QPV^{N-L}W_2|\nu\rangle\ . \tag{2.2}$$

The above is the trace of a product of operators with

$$P=\tfrac{1}{2}(|+\rangle\langle+|+|-\rangle\langle-|)\ , \tag{2.3}$$

$$Q|\nu\rangle=|-\nu\rangle\ , \tag{2.4}$$

$|-\nu\rangle$ is a state with all spins reversed relative to $|\nu\rangle$. The advantage of introducing P and Q is that these operators have a convenient form in the Jordan-Wigner representation, which we are going to use.

As is well known V can be represented[8,9] as

$$V=(2s)^{M/2}V_1(K)V_2(K)\ , \tag{2.5}$$

where

$$V_1(K)=\exp\left[K\sum_{j=1}^{M}\sigma_j^x\right] \tag{2.6}$$

transfers from column to column (our transfer matrix propagates in the direction perpendicular to the substrate) and

$$V_2(K)=\exp\left[K\sum_{j=1}^{M}\sigma_j^z\sigma_{j+1}^z\right] \tag{2.7}$$

transfers within a column. (We use periodic boundary conditions in the M direction and M is taken to be even.) In the above, $K=J/T$ (the Boltzmann constant is set to unity), σ^x and σ^z are the appropriate Pauli matrices,[8] and s in (2.5) denotes $\sinh 2K$. In terms of these matrices

$$W_{1,2}=(2s)^{M/2}V_1(K_{1,2})V_2(K)\ , \tag{2.8}$$

$$P=\tfrac{1}{2}\prod_{k=1}^{M}(1+\sigma_k^z\sigma_{k+1}^z)=\lim_{R\to\infty}e^{-RM}V_2(R)\ , \tag{2.9}$$

$$Q=\prod_{k=1}^{M}\sigma^x\ . \tag{2.10}$$

We apply the Jordan-Wigner transformation in the form

$$\sigma_j^x=2C_j^{\dagger}C_j-1,\quad -\sigma_j^z=(-1)^n(C_j^{\dagger}+C_j)\ , \tag{2.11}$$

where $n=\sum_{i<j}C_i^{\dagger}C_i$. Here the operators C_j satisfy fermionic commutation relations. In terms of the C_j's we have

$$Q=(-1)^{n'}\ , \tag{2.12}$$

with $n'=\sum_{k=1}^{M}C_k^{\dagger}C_k$ being the total number operator of fermions in the system.

The evaluation of the trace in (2.2) can be done in the representation in which V is diagonal. The diagonalization of V proceeds in the standard way and is described in detail in Ref. 9, the notation of which we are using here. This procedure has to be performed separately for n' even (e) and odd (o). Then we have

$$Z_{+-}=Z_{+-}^{e}+Z_{+-}^{o}\ . \tag{2.13}$$

In the even subspace Q can be replaced by $+1$, whereas in the odd subspace $Q=-1$. It follows that

$$Z_{+-}^{e}=Z_{++}^{e},\quad Z_{+-}^{o}=-Z_{++}^{o}\ . \tag{2.14}$$

Here $Z_{++}=Z_{++}^{e}+Z_{++}^{o}$ is the partition function of a system similar to the one in Fig. 1, but with all the boundary spins up (or down, since $Z_{++}=Z_{--}$). With this notation, the free energy of the system depicted in Fig. 1 is obtained as

$$-\frac{F}{T}=\ln Z_{++}^{e}+\ln\left[1-\frac{Z_{++}^{o}}{Z_{++}^{e}}\right]\ . \tag{2.15}$$

The surface free energy per spin (or surface tension) is expressed as

$$-\frac{f}{T}=\lim_{M\to\infty}\frac{1}{M}\ln\left[1-\frac{Z_{++}^{o}}{Z_{++}^{e}}\right]\ . \tag{2.16}$$

Here $Z_{++}^{o,e}$ are evaluated in the $N\to\infty$ limit. The calculation of $Z_{++}^{o,e}$ proceeds along the lines of Ref. 9, with the result

$$-2\ln\frac{Z_{++}^{o}}{Z_{++}^{e}}=\sum_{\sigma=1}^{M}\left[E\left[\frac{2\pi}{M}(\sigma-1)\right]-E\left[\frac{\pi}{M}(2\sigma-1)\right]\right]+\sum_{\sigma=1}^{M}\left[\kappa\left[\frac{2\pi}{M}(\sigma-1)\right]-\kappa\left[\frac{\pi}{M}(2\sigma-1)\right]\right]\ , \tag{2.17}$$

with

$$\cosh E(q)=cc^{*}+\cos q\ , \tag{2.18a}$$

$$e^{\kappa(q)}=(1+\cos q\cos a_q+c^*\sin q\sin a_q)[(c_1+s_1\cos a_q)(c_2+s_2\cos a_q)+e^{-2LE(q)}s_1s_2\sin^2 a_q]$$
$$+\sin a_q[\cos q\sin a_q+\sin q(s^*-c^*\cos a_q)][s_1(c_2+s_2\cos a_q)+e^{-2LE(q)}s_2(c_1-s_1\cos a_q)]\ , \tag{2.18b}$$

where a_q is defined by

$$\sinh E(q)\sin a_q=s\sin q\ , \tag{2.18c}$$

$$\sinh E(q)\cos a_q=c^*+c\cos q\ . \tag{2.18d}$$

In the above expressions $c^*=\cosh 2K^*$, $s^*=\sinh 2K^*$, $c_{1,2}=\cosh 2(K^*_{1,2}-K^*)$, and $s_{1,2}=\sinh 2(K^*_{1,2}-K^*)$; K^* is the dual of K defined by $e^{-2K^*}=\tanh K$.

Both $E(q)$ and $\kappa(q)$ are even functions of q and therefore can be expanded in the Fourier series,

$$E(q)=\sum_{m=0}^{\infty} e_m\cos mq\ ,$$
$$\kappa(q)=\sum_{m=0}^{\infty} b_m\cos mq\ . \tag{2.19}$$

Evaluating the two sums in (2.17), we get

$$-\frac{1}{M}\ln\frac{Z^0_{++}}{Z^e_{++}}=\sum_k (e_{kM}+b_{kM})\ , \tag{2.20}$$

where k in (2.20) runs over odd integers. It will be shown later that $e_{kM}\sim|\alpha|^{kM}$, $b_{kM}\sim|\beta|^{kM}$ with $|\alpha|,|\beta|<1$, therefore the $k=1$ term in the above sum dominates in the $M\to\infty$ limit. Given α and β, the free energy in (2.16) can be written as

$$-\frac{f}{T}=\lim_{M\to\infty}\frac{1}{M}\ln(1-e^{-M(a|\alpha|^M+b|\beta|^M)}$$
$$=\ln\max(|\alpha|,|\beta|)\ , \tag{2.21}$$

where a and b are some constants. Applications of the above formalism will be presented in the next sections.

III. THERMODYNAMICS OF WETTING FOR A SINGLE DEFECT LINE NEAR A WALL

In this section we mostly reproduce results of Ref. 3. In the special case of $J_2=J$ the expression for $\kappa(q)$ given in (2.18) simplifies considerably

$$e^{\kappa_A(q)}=c_1(1+\cos q\cos a_1)+s_1(\cos a_q+\cos q)$$
$$+(c_1c^*+s_1s^*)\sin q\sin a_q\ . \tag{3.1}$$

According to (2.20) and (2.21) we need the Fourier coefficients e_m and b_m of $E(q)$ given by (2.18) and $\kappa(q)$ given by (3.1). The Fourier series (2.19) can be written in terms of $z=e^{iq}$ as

$$E(z)=\tfrac{1}{2}\sum_m e_m(z^m+z^{-m})\ ,$$
$$\kappa_A(z)=\tfrac{1}{2}\sum_m b_m(z^m+z^{-m})\ . \tag{3.2}$$

The functions $E(z)$ and $\kappa(z)$ are analytic near $|z|=1$. We are interested in their singularities nearest to the unit circle. Let us denote the appropriate $|z|<1$ singularities by α and β, respectively, for $E(z)$ and $\kappa(z)$. (There are also singularities at α^{-1} and β^{-1} outside the unit circle). For large m, we have

$$\left|\frac{e_m\alpha}{e_{m-1}}\right|,\quad\left|\frac{b_m\beta}{b_{m-1}}\right|\simeq 1\ . \tag{3.3}$$

Finally, in terms of α and β,

$$e_M\sim|\alpha|^M,\quad b_m\sim|\beta|^M\ . \tag{3.4}$$

Let us first determine the singularity of $E(z)$ nearest to the unit circle. From (2.18)

$$E(z)=\ln\left\{cc^*+\frac{1}{2}(z+z^{-1})\right.$$
$$\left.+\left[\left[cc^*+\frac{z+z^{-1}}{2}\right]^2-1\right]^{1/2}\right\}, \tag{3.5}$$

$E(z)$ has a branch cut singularity at the point where the square root in (3.5) vanishes. We obtain

$$|\alpha|=cc^*-1-[(cc^*-1)^2-1]^{1/2}\ , \tag{3.6}$$

with α real and negative. By (2.18),

$$cc^*-1=\cosh E(\pi)\ , \tag{3.7}$$

and using the definition of c and c^*,

$$E(\pi)=2(K-K^*)\ . \tag{3.8}$$

Recall that the above expressions are considered here for $K>K^*$ (below T_c). Using (3.7) and (3.8) in (3.6), we get

$$|\alpha|=e^{-E(\pi)}\ . \tag{3.9}$$

Let us now determine the appropriate singularity of $\kappa_A(q)$ given by (3.1); $\kappa_A(q)$ has logarithmic singularities when the right-hand side (rhs) of (3.1) vanishes. With the notation

$$\delta=\tan\frac{a_q}{2},\quad w=\tan\frac{q}{2}\ , \tag{3.10}$$

the zeroes of the rhs of (3.1) are determined from

$$c_1(1+w^2\delta^2)+s_1(1-w^2\delta^2)+2w\delta\cosh 2K_1^*=0\ . \tag{3.11}$$

We need the solution of (3.11) nearest to the unit circle in the $z=e^{iq}$ plane. The relation between δ, w, and z is

$$\frac{1-w^2}{1+w^2}=\frac{z^2+1}{2z}\ , \tag{3.12}$$

$$\frac{\delta}{1-\delta^2}=\frac{sw}{(c^*+c)+(c^*-c)w^2}\ . \tag{3.13}$$

These equations are easily derived by using the definitions (3.10) of w and δ, and (2.18). In terms of z, (3.11) is a

fourth-order equation. It is easy to solve (3.11) for the variable $y=\delta w$. The appropriate solution for y is

$$y=-\exp(4K_1^*-2K^*)\ . \tag{3.14}$$

By employing (3.12)–(3.13) we obtain

$$w^2=\frac{sy^2+y(c^*+c)}{s+y(c-c^*)}\ . \tag{3.15}$$

With (3.15), z is finally determined by (3.12). For $T<T_c$ we have $w^2<0$ in (3.15). The solution $z=\beta$ closest to the unit circle is then given by

$$\beta=\frac{1-w^2}{1+w^2}-\left[\left[\frac{1-w^2}{1+w^2}\right]^2-1\right]^{1/2}\ . \tag{3.16}$$

The free energy of model A is obtained from (2.21) using (3.9) and (3.15). At the temperature defined by a $\alpha(T_w)=\beta(T_w)$ the second temperature derivative of the free energy has a jump. For $T<T_w$, $|\beta|>|\alpha|$. For $T>T_w$, $|\alpha|>|\beta|$, and $f=2(K-K^*)$, which is just the Onsager surface tension.[4] These results are illustrated in Fig. 2. The equation $\alpha=\beta$ for T_w reduces to

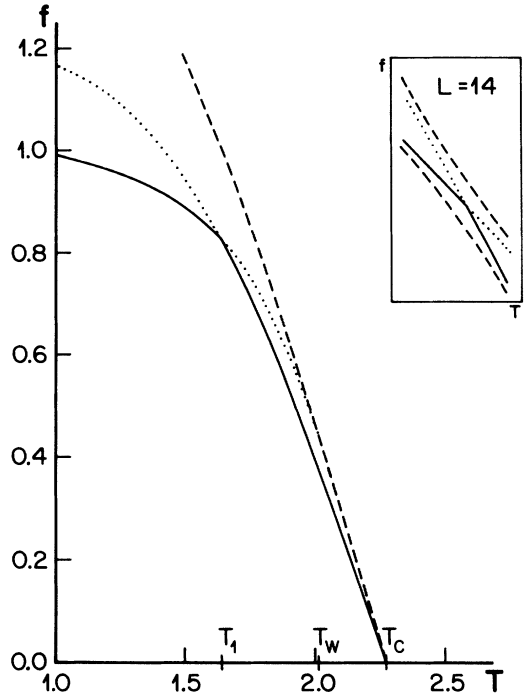

FIG. 2. Interfacial free energies per spin (surface tensions). The Onsager surface tension, of the 2D Ising model without defects is shown by the dashed line. The interfacial free energy of model AB, with $L=\infty$, is the solid line with a kink at $T_1(\simeq 1.62)$. Model B corresponds to dotted $(T<T_1)$-solid $(T>T_1)$ line, while model A corresponds to solid $(T<T_1)$-dotted $(T>T_1)$ line; a_1 and a_2 values for this figure are $a_1=0.5$, $a_2=0.6$. The inset shows magnification around the kink $(1.61\le T\le 1.63;\ 0.829\le f\le 0.849)$, for *finite* $L=14$. Two branches of f_{AB} correspond to the top and bottom dashed lines, see (5.4) *et seq.* When $L\to\infty$, the branches coincide to form a kink in f_{AB} (solid line in the inset).

$$\cosh 2K_1=\frac{c(c+1)+s(s-1)}{c(c+1)-s(s-1)}\ . \tag{3.17}$$

At T_w the interface depins from the substrate. This behavior was first obtained by Abraham.[3]

IV. TWO-DEFECT MODEL IN THE $L\to\infty$ LIMIT

For $a_2\neq 1$ we have to consider the full expression for $\kappa(q)$ given by (2.18). However, in the $L\to\infty$ limit we obtain

$$e^{\kappa_{AB}(q)}=e^{\kappa_A(q)}(c_2+s_2\cos a_q)\ . \tag{4.1}$$

In order to determine the free energy of model AB we have to locate the $|z|<1$ singularity of κ_{AB} nearest to the unit circle in the $z=e^{iq}$ plane. Such a singularity for κ_A has been found in the preceding section. Additional singularity is obtained by solving

$$c_2+s_2\cos a_q=0\ , \tag{4.2}$$

expressed in terms of $z=e^{iq}$. The solutions of this equation can be obtained in analogy with the ones considered in Sec. III. Denoting the appropriate solution by γ, we obtain

$$|\gamma|=-x-(x^2-1)^{1/2}\ , \tag{4.3}$$

where

$$x=\frac{cc^*-c_2(s_2^2s^4+1)^{1/2}}{s_2^2s^2-1}\ , \tag{4.4}$$

and γ is real and negative. By (2.21), the interfacial free energy, f_{AB}, of model AB can be written as

$$-\frac{f_{AB}}{T}=\ln\max(|\alpha|,|\beta|,|\gamma|)\ . \tag{4.5}$$

Let us introduce

$$-\frac{f_0}{T}=\ln|\alpha|\ , \tag{4.6a}$$

$$-\frac{f_A}{T}=\ln|\beta|\ , \tag{4.6b}$$

$$-\frac{f_B}{T}=\ln|\gamma|\ . \tag{4.6c}$$

Then

$$f_{AB}=\min(f_0,f_A,f_B)\ . \tag{4.7}$$

As mentioned in Sec. III f_0 is the surface tension of the homogeneous 2D Ising model $(a_1=a_2=1)$. Using (4.3)–(4.4), it is easy to show that below T_c, $f_0>f_B$. At T_c, $f_0=f_B$. According to the results of Sec. III, for $T<T_w$, $f_0>f_A$ and for $T_w\le T\le T_c$, $f_0<f_A$ (see Fig. 2). The first-order unbinding transition takes place at T_1 determined by

$$\gamma(T_1)=\beta(T_1)\ . \tag{4.8}$$

This corresponds to $f_A=f_B$. Using the analytic expressions for β and γ given by (3.15)–(3.16) and (4.3)–(4.4), relation (4.8) leads to

$$\left[\frac{x_1}{x_2}\right]^2=\frac{cs(1-x_1^2)-(c+sx_1^2)}{cs(1-x_1^2)-(s+cx_1^2)}\ , \tag{4.9}$$

where $x_i=\tanh(a_iJ/T)$ $(i=1,2)$. In the limit $a_2=1$ (4.9) reduces to

$$x_1^2=\frac{s(s-1)}{c(c+1)}\ , \tag{4.10}$$

which is equivalent to (3.17). All the above results are depicted in Fig. 2 (the inset will be discussed in Sec. V). For f_{AB} we finally have

$$f_{AB}=\begin{cases} f_A, & T\le T_1, \\ f_B, & T_1\le T\le T_c\ . \end{cases} \tag{4.11}$$

At T_1, f_{AB} has a kink; its first derivative with respect to T is discontinuous. The magnitude of this discontinuity determines the latent heat associated with the first-order transition.

The first-order transition at T_1 corresponds to a sudden jump of the interface (localized at the substrate at $T=0$) to the defect line at $L(\to\infty)$. The detailed study of this jump will be carried out in Sec. VII, whereas the shape of the magnetization profile will be discussed in Sec. VIII.

V. FINITE-SIZE EFFECTS FOR THE TWO-DEFECT MODEL

Expression (2.18) for κ allows us to study the effect of finite L on the first-order transition. By doing so we can verify the predictions of the general finite size scaling theory.[5] We will be interested in the asymptotic behavior (for model AB) close to T_1, with L large but finite. In this limit the condition for vanishing of e^{κ} in (2.18) can be expressed as

$$e^{\kappa_A}(c_1+s_2\cos q_q)=P_0e^{-2LE(q)}\ . \tag{5.1}$$

Here the coefficient of $e^{-2LE(q)}$,

$$\begin{aligned} P_0=s_2\sin a_q[&\sin a_q(s_1+c_1\cos q) \\ &+\sin q(\sinh 2K_1^*-\cosh 2K_1^*\cos q)]\ , \end{aligned} \tag{5.2}$$

as well as $E(q)$, are defined in (2.18) and are evaluated at $T=T_1$. In order to study the form of the rounded singularity (kink) of f_{AB} at T_1, we employ the method of Ref. 10. For $T\simeq T_1$ and large L, (5.1) reduces to

$$(z-\beta)(z-\gamma)=Pe^{-2LE}\ , \tag{5.3}$$

where $P\propto P_0$. From this we obtain the two roots

$$z_\pm=\tfrac{1}{2}\{(\beta+\gamma)\pm[(\beta-\gamma)^2+4Pe^{-2LE}]^{1/2}\}\ . \tag{5.4}$$

These resolutions correspond to the two branches of the free energy shown in the inset in Fig. 2 (solid-dashed lines). The true finite L free energy of model AB corresponds to the branch z_+ in (5.4). The gap between the two branches at T_1 behaves according to

$$\Delta f\propto e^{-LE}\ . \tag{5.5}$$

Away from T_1, in the strict $L\to\infty$ limit,

$$z_+=\tfrac{1}{2}[(\beta+\gamma)+|\beta-\gamma|]=\max(\beta,\gamma)\ . \tag{5.6}$$

For the $L=\infty$ free energy we have

$$f_{AB}=\tfrac{1}{2}[(f_A+f_B)-|f_A-f_B|]=\min(f_A,f_B)\ . \tag{5.7}$$

The "mixing" of the two free-energy branches as a mechanism of a finite-size rounding, given by (5.4), is similar to that predicted phenomenologically for bulk Ising models in cylindrical geometries.[5,10]

Some remarks concerning the crossover length scale E^{-1} in (5.5) are due. This length is not one of the obvious bulk quantities like the correlation length or the inverse surface tension. (The latter length scale enters bulk first-order transition scaling for Ising strips.[5]) Indeed, $E(z)$ as given by (2.18) is the Onsager function, however, it is evaluated at $T=T_1$ and $z\equiv e^{iq}=\beta=\gamma$. (It reduces to the Onsager surface tension for $z=\alpha$.) Solid-on-solid model calculations yield a more transparent interpretation of this length (see Sec. VII and VIII).

VI. THE SOLID-ON-SOLID MODEL FORMULATION. INTERFACIAL FREE ENERGY

The solid-on-solid (SOS) approximation has been introduced to model the low-temperature properties of Ising models.[11] It has been used[12] to describe the wetting transition in $d=2$. As will be demonstrated below, the qualitative features of the results of the rather complicated calculations in Sec. II–V can be obtained with less effort if the RSOS formulation of the Ising model is used. The relative simplification of the calculations in the RSOS model will enable us to obtain closed form expressions for the average distance of the interface from the substrate as well as for the magnetization profile. The calculation of these quantities for the Ising model has been carried out for model A only,[3] by employing sophisticated mathematical techniques. The limitation of the SOS or RSOS models is that for example the high- and low-temperature properties cannot be studied simultaneously. (The high-temperature phase does not exist in the SOS formulation.) T_c of the Ising model formally corresponds to $T=\infty$ in the SOS models. However, when typically low-T phenomena like wetting are to be studied, the essential physics can be grasped in the simplified formulation.

In this section we rederive the free energy of model AB in the RSOS formulation, both for finite L and the infinite-L limit. The SOS and RSOS models for the problem studied in this work have the following Hamiltonian:

$$H=J\sum_{i=1}^{M-1}|h_i-h_{i+1}|-u\sum_{i=1}^{M}\delta_{h_i,0}-v\sum_{i=1}^{M}\delta_{h_i,L},\quad J>0\ . \tag{6.1}$$

Here the variables h_i assume non-negative integer values, $h_i=0,1,2,\ldots$. The attractive substrate favors the configuration with $h_i=0$ $(i=1,2,\ldots,M)$, by reducing the energy by $u>0$ for every $h_k=0$. The third term in (6.1), with $v>0$, is minimal if all the h_i's are equal to L. As illustrated in Fig. 3, an SOS configuration $\{h_i\}$ corresponds to an Ising configuration with all the spins between the substrate and the interface being $-$, while all

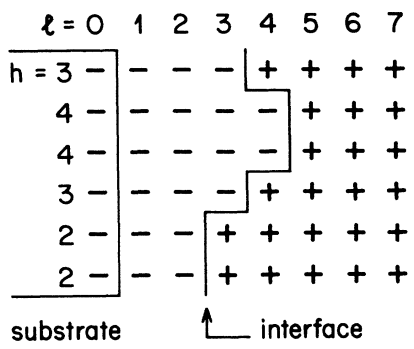

FIG. 3. Illustration of the correspondence between the states of the Ising spins (± 1), without overhangs and bubbles, and RSOS configurations of the interface separating $-$ and $+$ regions. The distance of the interface from the substrate is measured by the variables h. Neighboring h values can differ by at most one step in the RSOS model. Configurations of the interface are uniquely specified by the set of $\{h_i\}$.

the remaining spins being $+$. Thus, the SOS approximation eliminates Ising configurations with overhangs and bubbles which are believed to be irrelevant for wetting. If the difference of neighboring h_i's is allowed to have the values $0,\pm 1$ only, then (6.1) defines the RSOS model. If this difference is not restricted, (6.1) represents the SOS model. Since the actual calculations are simpler in the RSOS model while the qualitative properties are identical, we use the RSOS version in the following. We analyze model (6.1) by using the transfer matrix method.[11,12] The transfer matrix is labeled by the h values and a standard nonsymmetric choice for the RSOS model is

$$V_{hh'}=t^{|h-h'|^{\infty}}y^{\delta_{h,0}}w^{\delta_{h,L}}\ , \tag{6.2}$$

where $t=\exp(-J/T)$, $y=\exp(u/T)$, and $w=\exp(v/T)$. The discrete spectrum of V consists of zero, one or two eigenvalues which can be determined as follows. The right eigenfunctions of the discrete spectrum must be of the form[12]

$$\psi_h^R=\begin{cases} Ae^{-\mu h}+Be^{-\mu(2L-h)}, & h\le L, \\ Ce^{-\mu h}, & h\ge L. \end{cases} \tag{6.3}$$

Continuity at $h=L$ requires

$$A+B=C\ . \tag{6.4}$$

Substituting ψ_h in $\sum_{h'}T_{hh'}\psi_{h'}=\lambda\psi_h$, we obtain the consistency conditions at $h=L$ and $h=0$, respectively,

$$\lambda(A+Be^{-2\mu L})=y[A+Be^{-2\mu L}+t(Ae^{-\mu}+Br^{-\mu(2L-1)})]\ , \tag{6.5a}$$

$$\lambda(A+B)=w[t(Ae^{\mu}+Be^{-\mu})+(A+B)(1+te^{-\mu})]\ , \tag{6.5b}$$

while the eigenvalue equation for $h\neq 0,L$ leads to

$$\lambda=1+2t\cosh\mu\ . \tag{6.6}$$

The homogeneous system of equations (6.5) has a nontrivial solution for A and B if the determinant of the system vanishes. In the $L\to\infty$ limit this condition is equivalent to

$$(y+yte^{-\mu}-\lambda)(2wte^{-\mu}+w-\lambda)=0\ . \tag{6.7}$$

We seek solutions of the system (6.6)–(6.7) for $\mu(t;w,y),\lambda(t;w,y)$, satisfying $\mu>0$. It is easy to show that any eigenvalue of V which corresponds to the continuous part of the spectrum[13] is smaller then any solution λ of (6.6)–(6.7) (provided it exists). The free energy of the system is then given by the larger of the two solutions for λ. For fixed y and w we have

$$-\frac{\tilde{f}_{AB}}{T}=\begin{cases} \ln\lambda_a=\ln[y(1+te^{-\mu_a})], & t\le t_1, \\ \ln\lambda_b=\ln[w(1+2te^{-\mu_b})], & t\ge t_1. \end{cases} \tag{6.8}$$

At $t=t_1$ and $\mu=\mu^*$ given by

$$y(1+t_1e^{-\mu^*})=w(1+2t_1e^{-\mu^*})=1+2t_1\cosh\mu^*\ , \tag{6.9}$$

$\tilde{f}_{AB}$ has a kink. [The second equation in (6.9) is obtained by using (6.6).] The first equation in (6.9) can be solved for μ^*,

$$\frac{y-w}{t_1(2w-y)}=e^{-\mu^*}\le 1\ . \tag{6.10}$$

By substituting in the second equation in (6.9), t_1 can be expressed in terms of y and w as

$$t_1=\frac{[w(y-w)(y-1)]^{1/2}}{2w-y}\ . \tag{6.11}$$

Thus (6.10) implies that the first-order transition in the RSOS model exists provided

$$1\le\frac{y}{w}\le\frac{3}{2}\ . \tag{6.12}$$

The borderline case, $y=w$ is equivalent to $a_1=a_2$; in this case $T_1=0$. For $y/w=\frac{3}{2}$ (i.e., $e^{-\mu^*}=1$) we have $t_1=1$, $T_1=\infty$.

If the first expression on the rhs of (6.8) is continued to the region with $1\ge t>t_1$, then $-T\ln\lambda_a$ determines the free energy of a model with $w=1$, $v=0$. This is the RSOS version of model A. There is a continuous wetting transition in this case, at $\mu=0$ (the bound state reaches the edge of the continuous spectrum); t_w is then obtained by equating the first and third expressions in (6.9) at $\mu=0$,

$$y=\frac{1+2t_w}{1+t_w}\ . \tag{6.13}$$

For $t_w=1$ (i.e., $T_w=\infty$), $y=\frac{3}{2}$.

If the second expression on the rhs of (6.8) is continued into the region $0\le t<t_1$, then $-T\ln\lambda_b$ determines the free energy of the symmetric RSOS model.[3,12] This is an RSOS model B, in which the values of the integer variables h_i are not restricted, and the Hamiltonian is

$$H=J\sum_i |h_i-h_{i+1}| - v\sum_i \delta_{h_{i,0}} . \tag{6.14}$$

In the symmetric RSOS model there is a continuous wetting transition only for $t_w=1$, $T_w=\infty$, $w=1$. (The Ising equivalent of the model B has the free energy[3] drawn by a dotted line for $T\le T_1$ and by a full line for $T\ge T_1$ in Fig. 2.)

The effect of finite L on the first-order unbinding transition can be studied analogously to that described in Sec. V. The condition for the vanishing of the determinant of the system of equations (6.5) for t close to t_1 and large (but finite) L can be written as

$$(\lambda-\lambda_a)(\lambda-\lambda_b)=\tilde{P}e^{-2\mu^* L} . \tag{6.15}$$

Here λ_a,λ_b are given by (6.8) and

$$\tilde{P}=4wyt_1^2\cosh^2\mu^* . \tag{6.16}$$

From here on the discussion of the finite-L effects is identical to the one given in Sec. V and will not be repeated. The finite length scale analogous to E^{-1} in (5.3) is now $(\mu^*)^{-1}$. The interpretation of this length scale will be clarified by further RSOS calculations in Secs. VII and VIII.

VII. AVERAGE INTERFACE DISPLACEMENT

The average distance of the interface from the substrate will be calculated using the RSOS formulation of model *AB*. As discussed in Sec. VI the position of the interface separating the + and − phases of the SOS model in the nonwet regime is determined once the values of all the integer variables h_i are specified (see Fig. 3). The average distance of the interface from the substrate is therefore given by

$$\langle h_k\rangle=\frac{\sum\langle h_0|V^k\hat{h}_kV^{M+1-k}|h_M\rangle}{\sum\langle h_0|V^{M+1}|h_M\rangle} . \tag{7.1}$$

Here $|h_i\rangle$ is the state vector of the ith layer. The state of the zeroth layer is fixed (typically at $h_0=0$) and the summations in (7.1) are carried out over all the possible states of the Mth layer. Using the spectral representation of V in the thermodynamic limit ($M\to\infty$) (7.1) becomes

$$\langle h\rangle=\langle\psi^L|\hat{h}|\psi^R\rangle . \tag{7.2}$$

In (7.2), $|\psi^R\rangle$ and $\langle\psi^L|$ stand for the right and left eigenstates of the nonsymmetric matrix V, corresponding to the largest eigenvalue. In the "h" representation [when $|\psi^R\rangle$ is given by (6.3)] the effect of the operator $\hat{h}$ on the rhs of (7.2) is multiplication by an integer number h. V can be symmetrized by a similarity transformation

$$V=SV_sS^{-1} , \tag{7.3}$$

where S is diagonal with $S_{hh'}=\epsilon_h\delta_{hh'}$, and

$$\epsilon_h=\begin{cases} y^{1/2}, & h=0,\\ w^{1/2}, & h=L,\\ 1, & \text{otherwise.}\end{cases} \tag{7.4}$$

In terms of ψ_0, the eigenfunction of V_s,

$$\langle h\rangle=\langle\psi_0|S^{-1}\hat{h}S|\psi_0\rangle , \tag{7.5}$$

$|\psi_0\rangle$ can be easily calculated once $|\psi^R\rangle$ is known, see (6.3), with the constants A, B, C determined by (6.4), (6.5), and by the normalization condition. Omitting the details of these straightforward but lengthy calculations, we only quote some results. First, consider $\langle h\rangle$ at $t=t_1$ for large finite L. We have

$$\psi_0(h)=\beta e^{\mu^* L}\epsilon_h\phi_0(h) , \tag{7.6}$$

$$\phi_0(h)=\begin{cases}\left[\left[\dfrac{y}{w}\right]^{1/2}e^{-\mu^* L}+e^{-2\mu^*(L-h)}\right]e^{-\mu^* h}, & h\le L,\\ \left[\left[\dfrac{y}{w}\right]^{1/2}e^{-\mu^* L}+1\right]e^{-\mu^* h}, & h\ge L,\end{cases} \tag{7.7}$$

where

$$\beta\equiv\left[\frac{w(e^{2\mu^*}-1)}{2(e^{2\mu^*}-1)+y+2w}\right]^{1/2} . \tag{7.8}$$

With the above results, (7.5) can be evaluated, with the leading order result

$$\langle h\rangle\sim L . \tag{7.9}$$

This shows that at the first-order transition the interface becomes pinned to the defect line. The average distance of the interface measured from the wall diverges, the interface unbinds from the substrate, but it *does not become delocalized.*

At $t=t_1$, $L\to\infty$ the value of $\langle h\rangle$ is expected to jump from a finite value to infinity. This finite can be evaluated by repeating the calculation for $t\to t_1^-$ but with $L\equiv\infty$. One obtains

$$\langle h\rangle\sim 1/\mu^* . \tag{7.10}$$

Relation (7.10) then suggests an interpretation of the finite-size length scale $(\mu^*)^{-1}$ in the RSOS model, and possibly $(E)^{-1}$ in the Ising model.

If $\langle h\rangle$ is evaluated with $v=0$ (the RSOS analog of model *A*), it is found to diverge continuously at t_w, the temperature of the wetting transition. As discussion earlier, $\mu=0$ at t_w. For $t\lesssim t_w$, $\langle h\rangle\sim 1/\mu$. [By (7.10), the crossover from the first-order to second-order transition can, in principle, be investigated by taking the limit $v\to 0$, $w\to 1$ of the SOS results. Indeed, from (6.10) and (6.11) one obtains that in this limit $t_1=t_w=(y-1)/(2-y)$ and $\mu^*=0$.]

VIII. MAGNETIZATION PROFILE FOR THE RSOS MODEL

As discussed in Sec. VI there is a one-to-one correspondence between the configurations of the RSOS and the Ising model without overhangs and bubbles (see Fig. 3). This correspondence allows the calculation of the average magnetization of a column of spins in Figs. 1 and 3 as a function of the distance from the substrate within the RSOS formulation. For the Ising case this profile has

been calculated in Ref. 3 using a rather complicated approach (for model A only). In this section we first derive the result for the RSOS profile of model A (compare Ref. 3) and then calculate it for model AB. Because of the analogy between the RSOS and Ising models it is easy to see that the average value of the magnetization in the lth column (see Fig. 3) can be obtained from

$$Z=\sum \langle h_0 \mid (VQ)^{M+1} \mid h_M \rangle \tag{8.1}$$

by differentiation with respect to the applied fieldlike variable H which enters the matrix elements of a diagonal matrix Q defined by $Q_{hh'}=\eta_h \delta_{hh'}$ with

$$\eta_h=\begin{cases} e^{H}, & h<l, \\ e^{-H}, & h\geq l. \end{cases} \tag{8.2}$$

This follows from the above mentioned correspondence between the SOS and Ising configurations. A column vector with $h=3$ for example corresponds to a layer of $+$, $-$ spins as

$$h_3=\begin{bmatrix} 0 \\ 0 \\ 0 \\ 1 \\ 0 \\ \vdots \end{bmatrix} \leftrightarrow s_{h_3}=\begin{bmatrix} - \\ - \\ - \\ - \\ + \\ \vdots \end{bmatrix} . \tag{8.3}$$

The matrix Q appropriately weighs the $+$ and $-$ spins in the layer s_h. The matrix element in (8.1) can be easily evaluated using the results of Sec. VII. For $v=0$ the normalized ground-state eigenfunction ψ_0 of the symmetric transfer matrix is

$$\psi_0(h)=\tilde{\epsilon}_h \left[\frac{1}{y}+\frac{1}{e^{2\mu}-1} \right]^{1/2} e^{-\mu h} \quad (v=0) , \tag{8.4}$$

with

$$\tilde{\epsilon}_h=\begin{cases} (1/y)^{1/2}, & h=0, \\ 1, & h\neq 0. \end{cases} \tag{8.5}$$

[The matrix S in (7.3) has diagonal elements $\tilde{\epsilon}_h$.] In the thermodynamic limit we finally obtain, analogously to (7.5),

$$m_l=\langle s_l \rangle = 1-\frac{2ye^{-\mu l}}{1+e^{-2\mu}(y-1)} . \tag{8.6}$$

Here m_l is the magnetization of a layer at a distance l from the substrate; μ in (8.6) is a solution of

$$y(1+te^{-\mu})=1+t(e^{\mu}+e^{-\mu}) \tag{8.7}$$

[see discussion following Eq. (6.12)]. For model A, a continuous wetting transition takes place at t_w [given by (6.13) or (8.7) with $\mu=0$]. Indeed, with $\mu=0$, (8.6) yields $m_l=-1$ for all l. On the other hand for finite $\mu>0$ ($t<t_w$), $m_l\cong 1$ for $l\gg 1/\mu$. Clearly μ^{-1} characterizes the size of the $-$ layer. Below the transition, m_l changes sign at l^* which can be obtained from (8.6),

$$l^*=-\frac{l}{2\mu}\ln\left[\frac{1+e^{-2\mu(y-1)}}{2y}\right]\sim\frac{\ln 2}{2\mu} . \tag{8.8}$$

The calculation of the profile for model AB is now straightforward. Only ψ_0 and S are changed compared to (8.4) and (8.5). Their appropriate forms are given by (7.4), (7.6), and (7.7). First we consider the limit of L large but finite, at $t=t_1$, $\mu=\mu^*$. Denoting $l=\alpha L$, we obtain for $\alpha<1$ ($L\gg 1$)

$$m_l=\frac{\beta^2}{e^{2\mu^*}-1}\left[\frac{y}{w}(1-e^{2\mu^*}e^{-2\mu^*\alpha L}) -2-2e^{-2\mu^* L(1-\alpha)}\right] . \tag{8.9}$$

The equation $m_l=0$ has no solution for α, so $m_l<0$ in this limit. A similar calculation with $\alpha>1$ ($L\gg 1$) yields

$$m_l=\frac{\beta^2}{e^{2\mu^*}-1}\left[\frac{y}{w}\left[1+\frac{2}{y}(e^{2\mu^*}-1)\right] +2-2e^{-2\mu^* L(\alpha-1)}\right] . \tag{8.10}$$

Solving for $m_l=0$, we get

$$\alpha^*=1+\frac{1}{L}\left[1+\frac{2}{\mu^*}\ln\left[1+\frac{y}{2w}+\frac{1}{w}(e^{2\mu^*}-1)\right]\right] . \tag{8.11}$$

The quantity $l^*=\alpha^* L$ at which m_{l^*} changes sign plays a role similar to $\langle h \rangle$. At t_1, l^* diverges $\propto L$. On the other hand, the calculation with $L\equiv\infty$, while $t\rightarrow t_1^-$, yields

$$l^*\sim 1/\mu^* . \tag{8.12}$$

At the sharp $L\equiv\infty$ first-order transition, l^* jumps from a finite value proportional to $(\mu^*)^{-1}$ to infinity. This gives another interpretation of the finite length scale $(\mu^*)^{-1}$.

IX. CONCLUSIONS

We have presented a model of interface unbinding. This unbinding transition becomes sharp first-order in the limit $L\rightarrow\infty$. Thermodynamic properties of this transition have been calculated exactly by using the Ising or the RSOS formulation of the model. Finite-L effects have been analyzed and predictions of finite-size scaling theory at first-order transitions verified.

As long as L is finite, the phase transition is not sharp. [In fact, for $L<\infty$ there is an unbinding transition from the two defect structure as a whole, at a higher temperature, at $T_c-O(L^{-1})$, see Ref. 6 for details.] In the "contact angle" or droplet shape interpretation of wetting, due to Cahn (see Ref. 14), the presence of the second defect at L, will manifest itself in a rapid variation of the droplet form at height L, as T is varied near T_1. The $L\rightarrow\infty$ limit, however, does not "commute" with the fixed average coverage constraint needed for the droplet-

shape interpretation of wetting.[15] Indeed, for fixed coverages, model A will be recovered in the strict $L \to \infty$ limit. Thus, the first-order unbinding transition described in this work has no appropriate Young's equation associated with it. In summary, a consequence of our analysis is that defects or imperfections far from the substrate can produce a practically sharp first-order unbinding transition.

ACKNOWLEDGMENTS

Research by V.P. and N. M. S. has been supported by the U. S. National Science Foundation under Grant No. DMR-86-01208, and by the Petroleum Research Fund, administered by the American Chemical Society, under Grant No. ACS-PRF-18175-G6. This financial assistance is gratefully acknowledged.

[1]For recent reviews see, M. E. Fisher, J. Chem. Soc., Faraday Trans. **2**, **82**, 1569 (1986); V. Privman and N. M. Svrakic, J. Stat. Phys. **51**, 1111 (1988).

[2]Recent reviews on wetting are D. Sullivan and M. M. Telo da Gama, *Fluid Interfacial Phemomena* (Wiley, New York, 1985); P.-G. de Gennes, Rev. Mod. Phys. **57**, 827 (1985); S. Dietrich, in *Phase Transitions and Critical Phenomena,* edited by C. Domb and J. Lebowitz (Academic, London, 1988), Vol. 12.

[3]D. B. Abraham, Phys. Rev. Lett. **44**, 1165 (1980); J. Phys. A **14**, L369 (1981). These publications present exact results for models A and B, respectively, in our notation.

[4]For a review of exactly solvable models with second order phase transitions, see R. J. Baxter, *Exactly Solved Models in Statistical Mechanics* (Academic, New York, 1982).

[5]V. Privman and M. E. Fisher, J. Stat. Phys. **33**, 385 (1983).

[6]Some of the results presented in this work have already been published, G. Forgacs, N. M. Svrakic, and V. Privman, Phys. Rev. B **37**, 3818 (1988). Further studies, including effects of disorder at the defect at L, have been reported by G. Forgacs and Th. M. Nieuwenhuizen J. Phys. A **21**, 3871 (1988).

[7]J. W. Cahn, J. Chem. Phys. **66**, 3667 (1977).

[8]T. D. Schultz, D. Mattis, and E. H. Lieb, Rev. Mod. Phys. **36**, 856 (1964).

[9]G. Forgacs, W. Wolff, and A. Suto, J. Phys. A **19**, 1899 (1986).

[10]V. Privman and L. S. Schulman, J. Phys. A **15**, L231 (1982); J. Stat. Phys. **29**, 205 (1982).

[11]H. N. V. Temperley, Proc. Cambridge Phil. Soc. **48**, 683 (1952); H. N. V. Temperley, Phys. Rev. **103**, 1 (1956); E. Mueller-Hartmann and J. Zittartz, Z. Phys. B **27**, 261 (1977).

[12]S. T. Chui and J. D. Weeks, Phys. Rev. B **23**, 2438 (1981); J. M. J. van Leeuwen and H. J. Hilhorst, Physica **107A**, 319 (1981); T. W. Burkhardt, J. Phys. A **14**, L63 (1981); D. M. Kroll, Z. Phys. B **41**, 345 (1981); J. T. Chalker, J. Phys. A **14**, 2436 (1981).

[13]For a discussion of the continuous spectrum of V see, G. Forgacs, J. M. Luck, Th. M. Nieuwenhuizen, and H. Orland, Phys. Rev. Lett. **57**, 2184 (1986), J. Stat. Phys. (to be published); V. Privman, G. Forgacs, and H. L. Frisch, Phys. Rev. B **37**, 9897 (1988).

[14]M. R. Moldover and J. W. Cahn, Science **207**, 1073 (1980).

[15]For a discussion of the connection between drops, macroscopic liquid layers, and the values of $\langle h \rangle$, see the review by Dietrich (Ref. 2).